



**University of
Zurich^{UZH}**

**Zurich Open Repository and
Archive**

University of Zurich
University Library
Strickhofstrasse 39
CH-8057 Zurich
www.zora.uzh.ch

Year: 2018

Dye Purification. An Image-processing Technique for the Digital Restoration of Chromogenic Film

Trumpy, Giorgio ; Flueckiger, Barbara

Abstract: The majority of color film heritage shot between the 1940s and the 1980s is faded. The bleaching of dyes cannot be reversed with chemical methods. Digital technologies can provide the means to recover faded colors. Still, the result of the digital unfading depends on the amount of residual color present in the film, the quality of the image capture operation, and the efficacy of the digital image processing. This paper first discusses the strategies to best capture the residual color information in the film, and then presents a processing method that consistently improves the digital restoration of the most common type of fading: the bleaching of the cyan dye that results in the typical pinkish cast of historical photographs.

DOI: <https://doi.org/10.1109/CVCS.2018.8496726>

Posted at the Zurich Open Repository and Archive, University of Zurich

ZORA URL: <https://doi.org/10.5167/uzh-158941>

Conference or Workshop Item

Published Version

Originally published at:

Trumpy, Giorgio; Flueckiger, Barbara (2018). Dye Purification. An Image-processing Technique for the Digital Restoration of Chromogenic Film. In: 2018 Colour and Visual Computing Symposium (CVCS), Norway, 19 September 2018 - 20 September 2018, CVCS.

DOI: <https://doi.org/10.1109/CVCS.2018.8496726>

Dye purification: an image-processing technique for the digital restoration of chromogenic film

Giorgio Trumpy
Department of Film Studies
University of Zurich
Zurich, Switzerland
giorgio@trumpy.eu

Barbara Flueckiger
Department of Film Studies
University of Zurich
Zurich, Switzerland
baflueckiger@gmail.com

Abstract—The majority of color film heritage shot between the 1940s and the 1980s is faded. The bleaching of dyes cannot be reversed with chemical methods. Digital technologies can provide the means to recover faded colors. Still, the result of the digital unfading depends on the amount of residual color present in the film, the quality of the image capture operation, and the efficacy of the digital image processing. This paper first discusses the strategies to best capture the residual color information in the film, and then presents a processing method that consistently improves the digital restoration of the most common type of fading: the bleaching of the cyan dye that results in the typical pinkish cast of historical photographs.

Keywords—Cinematography, Color, Optical microscopy, Motion pictures, Multispectral imaging.

I. INTRODUCTION

The first chromogenic negative-positive stock was introduced in the early 1940s. After decades of technological attempts to efficiently record and reproduce colors, it was finally possible to make multiple color copies of the same picture with a straightforward process. This important innovation greatly increased the production of photographic images, but those images were soon found to be constituted by fugitive dyes. It was only in the early 1980s, under the pressure of newborn film preservation initiatives, that manufacturers began producing film stocks with more stable dyes [1].

However, the majority of color pictures shot between the 1940s and the 1980s is faded. The bleaching of dyes cannot be reversed with chemical methods, but digital technologies can provide the means to recover faded colors [2-4]. The success of such recovery depends on the amount of residual color still present in the film, the quality of the image capture operation [5], and the efficacy of the digital image processing.

After describing the dye fading and the imaging systems that best capture the residual color information, this paper presents an image-processing method that improves the digital reconstruction of faded film colors.

II. CHROMOGENIC FILM AND DYE FADING

A chromogenic film is a three-layer system that, after exposure and processing, has a different image recorded in each layer. The images are constituted by cyan, magenta and yellow dyes (*subtractive colors*), which modulate the long, medium and short visible wavelengths respectively. This mechanism is quantitatively described by the *spectral densities* (see for example the spectra reported at the top of Fig. 1).

Photographic dyes have smooth transitions and do not only absorb light in their pertinent spectral region; they partly absorb light also in the adjacent regions. The most intense of these “side absorptions” (indicated by the darker areas in the plots of Fig. 1) are usually given by the cyan dye in the medium wavelengths, and by the magenta dye in the short wavelengths. The yellow dye, on the other hand, generally does not exhibit strong side absorptions [6].

Film colors deteriorate with time. ‘Dark fading’ refers to dye loss due to the action of temperature and humidity. In most chromogenic print films used in cinematography, dark fading typically develops affecting the cyan dye first; then it affects the yellow dye, leaving the typical reddish/pinkish cast of historical photographs [1].

III. FILM SCANNING AND ‘COLOR SEPARATION’

To acquire colors, professional film scanners use three spectral bands, which are mainly determined either by the emissions of a composite light source (e.g. three LEDs), by some filtering system (e.g. Color Filter Array), or by the combination of both. Several scanner manufacturers opt for spectral bands that do not overlap, considerably deviating from the human eye’s sensitivities (see for example the spectral bands reported in Fig. 3). These spectral bands exclude those regions where typical film dyes do not exhibit their absorption peaks and their absorbances largely overlap. Such choice minimizes the effect of the side absorptions, so the image of each spectral band is mostly determined by one dye only. The resulting digital images are said to have high “color separation”, which allows adjusting their colors more freely while grading, hence a more successful digital reconstruction of faded film colors can be achieved.

In the framework of the ERC Advanced Grant *FilmColors*, we developed a custom-made multispectral imaging system working in transmission geometry. The system has been devised to study the optical characteristics of historical film colors, and to design optical solutions that overcome the shortcomings of film scanners available on the market to date [7]. A linear variable interference band-pass filter selects spectral bands with around 18 nm FWHM from the emission of a *Light Emitting Plasma* bulb, and images are captured by a camera composed by a 16 megapixel full-frame monochrome CCD with dynamic range of around 70 dB equipped with a 65 mm f/2.8 macro lens. By opportunely positioning the band-pass filter, the spectral band’s position can be freely set between 400 and 720 nm. The distinctive feature of this multispectral system is that the *condensed* illumination typical of mechanical film projectors can be recreated. For the image acquisitions reported in this paper (section VII), ‘standard’ diffuse illumination is used instead, as it is the suitable illumination type for the digitization of nonscattering chromogenic film [8].

This work was supported by the research project *FilmColors* that benefits from an Advanced Grant from the European Research Council (ERC) under the European Union’s Horizon 2020 research and innovation programme (grant agreement n° 670446).

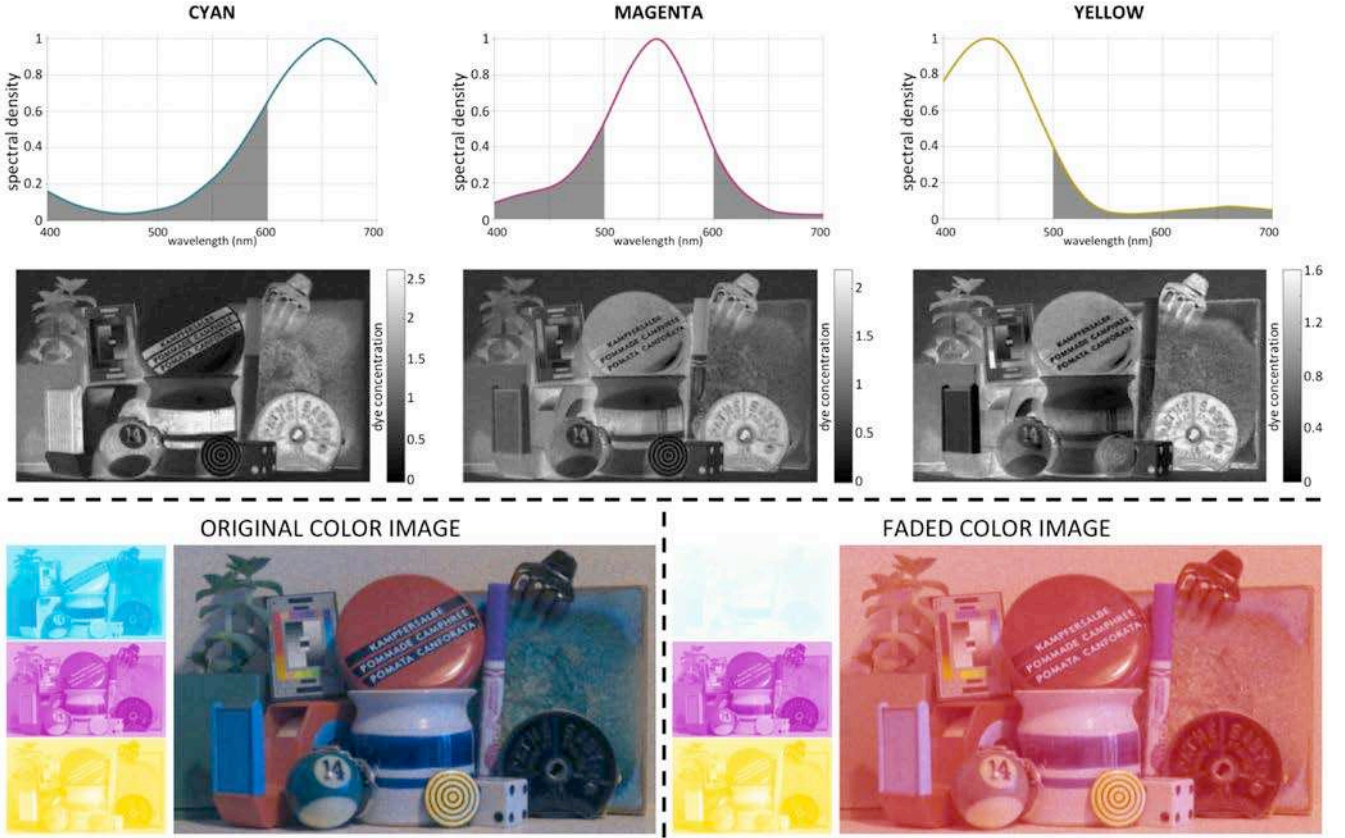


Fig. 1. Top: Spectral densities and concentration maps that compose the 'synthetic' hyperspectral image of a chromogenic film. Bottom-left: Color of the individual emulsion layers and overall colors of the film. Bottom-right: Colors after simulating the fading of the cyan dye.

IV. THE SCANNING OF FADED FILM

To illustrate the image-processing procedure for the digital reconstruction of faded film colors, we first construct a numerical example. A 'synthetic' hyperspectral transmittance image of a photographic film is assembled envisioning three overlapping dyed emulsions (C , M and Y), each of them characterized by the dye's spectral density ($SD(\lambda)$) and its corresponding concentration map ($K^{(x,y)}$). In accordance with the *Beer-Lambert* law, the absorbances of the film are calculated as follows:

$$A^{(x,y)}(\lambda) = K_C^{(x,y)} \times SD(\lambda)_C + K_M^{(x,y)} \times SD(\lambda)_M + K_Y^{(x,y)} \times SD(\lambda)_Y \quad (1)$$

The spectral densities and the concentration maps are displayed in the top part of Fig. 1; the images at the bottom-left show the resulting colors of the individual layers and the overall film on a D50 backlight [9][10]. The fading is modeled by a multiplying factor (0.05) that abates the concentrations of the cyan dye, recreating a typical level of 'dark fading' found in old photographic pictures. The resulting faded colors are shown at the bottom-right of Fig. 1. The spectral bands of a film scanner designed for high color separation (cf. section III) are modeled by three Gaussians with 20 nm FWHM and sensitivity peaks at 450, 550 and 650 nm (Fig. 3). The sensor is considered having *full well capacity* of $33'700 \text{ e}^-$ and *read noise* of 15 e^- , corresponding to a *dynamic range* of around 67 dB. A perfectly homogeneous illumination on the film is considered. The simulated image capture produces a 16-bit grayscale image for each spectral band (IMG_R , IMG_G and IMG_B). In the present paper we consider linear images that are normalized to the value of the unabsorbed light (white), so the image values correspond to the film transmittances.

V. DIGITAL UNFADING

To efficiently and consistently perform the digital unfading, we developed an automatic color correction method. A computer routine finds the transformation that minimizes the color difference between an input image and its corresponding *reference image* with target colors. Three *Look-Up Tables* (LUT), one for each color channel, are used to adjust the colors of the faded image. Each LUT is a curve defined by its black-value (1 variable), its white-value (1 variable) and two midpoints that can move up/down and left/right (2 variables each). The routine finds the optimal values for the eighteen variables (six for each LUT) through a multi-step minimization process based on the *Nelder-Mead simplex algorithm* [11]. The original unfaded colors of the numerical example presented in section IV are known (bottom-left of Fig. 1), so the automatic color correction of the digitized faded film can be run using this reference. The image to be unfaded is the result of the virtual digital capture described at the end of section IV. For the moment, we consider the simplest merging approach (we call it "simple merge") that assigns IMG_R to the R channel, IMG_G to the G channel, and IMG_B to the B channel to create a 16-bit RGB image.

The result of the automatic digital unfading is reported in Fig. 2: the transformation is constituted by the three one-dimensional LUTs; the colors of the 'unfaded image' cannot be considered a good result when compared to the reference colors before fading (Fig. 1); the pixel-by-pixel residual colorimetric distance from the original unfaded colors (Euclidean distance in the CIELAB space [12]) exhibits values higher than 20 ΔE units, which correspond to a strong color difference. No better result is achievable with the LUTs used to correct the image color.

VI. DYE PURIFICATION

To understand the reason behind the unsatisfactory result reported in Fig. 2, it is necessary to examine in detail the image capture of the faded film.

The absorbances of the three emulsion layers are plotted in Fig. 3, showing the variability of the dye concentrations across the image. The plot also displays the spectral bands of the color-imaging device. Due to the fading of the cyan dye, the image captured in the red spectral band (Fig. 3 – right plot at 650 nm) is a more or less equal mixture of all dyes, since the remaining cyan absorption and the side absorptions of the other two dyes have similar intensities. Hence, the acquired image in the red band (IMG_R) does not carry actual color information, and stretching its histogram will not lead to the restoration of the original absorbances of the cyan image.

However, the unfortunate situation of the cyan fading offers an opportunity: the yellow dye does not exhibit strong side absorptions, and the side absorption of the faded cyan dye in the middle wavelengths has become negligible. As a result, the image captured in the green band (Fig. 3 at 550 nm) corresponds almost exclusively to the magenta dye ($IMG_R \cong M$). This allows constructing the following described “dye purification” procedure.

In each spectral band, the absorbances of the individual dye layers combine additively (as in (1)). The residual information of the faded cyan dye can be extracted from the digital capture in two steps. First, the contribution of the magenta dye is subtracted from the image captured in the B band, in order to obtain the pure yellow dye image:

$$Y^* = IMG_B^* - (cf_1 \times IMG_G^*) \quad (2)$$

The “contamination factor” cf_1 quantifies the contribution of the magenta side absorption in the image captured in the B band. The asterisks indicate that the image values are converted to absorbances. In the second step, the contributions of the magenta and yellow dyes are subtracted from the image captured in the R band, so to obtain the pure cyan dye image:

$$C^* = IMG_R^* - (cf_2 \times IMG_G^*) - (cf_3 \times Y^*) \quad (3)$$

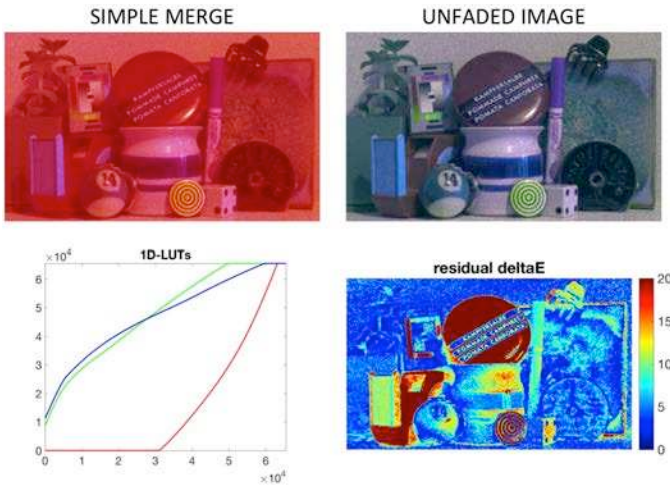


Fig. 2. Result of the digital unfading for the “simple merge”: input image (top-left), visual product of the digital restoration (top-right), LUTs that define the transformation (bottom-left), and the residual colorimetric distance from the original unfaded colors (bottom-right).

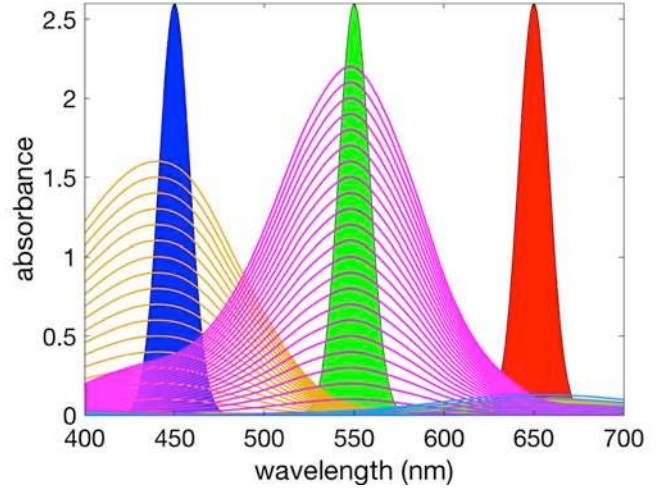


Fig. 3. Absorbances of yellow, magenta and cyan dyes after fading. The spectral bands of the modeled film scanner are overlaid as blue, green and red areas.

In the present numerical case, $cf_1 = 0.176$, $cf_2 = 0.058$ and $cf_3 = 0.064$. A new RGB image (we call it “pure merge”) can be constructed with the images captured in the G and B bands plus the transmittance image corresponding to the pure cyan dye ($IMG_{cyan} = 10^{-C^*}$). The automatic digital unfading described in section V is conducted a second time with the new RGB image. The new result is reported in Fig. 4; this time, the original colors are better recovered and the pixel-by-pixel residual colorimetric distance from the original unfaded colors is lowered.

VII. REAL CASE

The results of the numerical example presented in sections IV, V and VI demonstrated that the “dye purification” technique can potentially provide a great improvement to the digital reconstruction of faded chromogenic films. We now try to confirm this by testing the technique on the digitization and color reconstruction of a ‘real’ faded film. A film print from the collection of the *Deutsches Filminstitut* in Frankfurt (DIF 50 064) is selected for the test (Fig. 5): the ‘Kulturfilm’ (i.e. documentary film) “Frühling in den Vogesen” (GER 1942) printed on the newly introduced *Agfacolor Neu*.

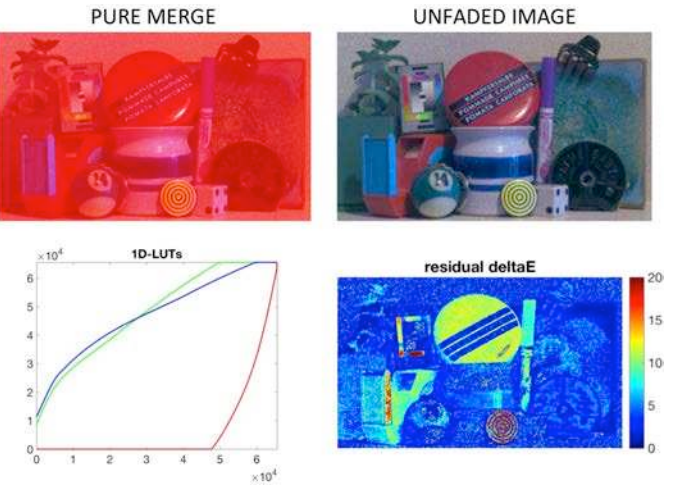


Fig. 4. Result of the digital unfading for the “pure merge”: input image (top-left), visual product of the digital restoration (top-right), LUTs that define the transformation (bottom-left), and the residual colorimetric distance from the original unfaded colors (bottom-right).

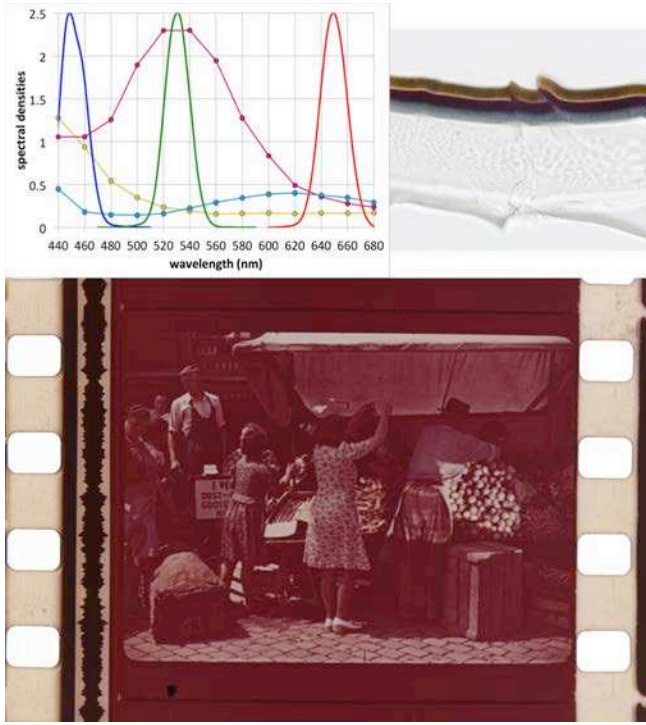


Fig. 5. *Kulturfilm* “Frühling in den Vogesen” (GER, 1942): color image of the faded film (bottom), microscopic image of a thin section from the film (top-right) and measured spectra of the individual emulsion layers (top-left). The plot also shows the spectral bands used to image the film frame.

The film exhibits the kind of fading that can be confronted with the “dye purification” technique: quite well preserved yellow and magenta dyes and a strongly – but not completely – faded cyan dye. The images of a film frame are captured with the multispectral imaging system described in section III selecting three spectral bands with sensitivity peaks at 450, 530, and 650 nm (Fig. 5 – top-left). Film transmittances were calculated through standard *flat-fielding correction*, referring to the unabsorbed illumination without film (*white*) and the image captured without light (*dark*).

To estimate the contamination factors in (2) and (3), it was necessary to measure the maximum absorbances of the individual constituent dyes. A viable way to directly measure them is to cut thin sections with a rotary microtome from a dark part of the film [13]. A 40-micron thickness is small enough for the section to fall on its side, displaying the layered structure of the film under the microscope (Fig. 5 – top-right). To preserve the film integrity, the sample was cut from a part that did not include the image or soundtrack, and did not notch the perforation holes. The section was analyzed at the microscope and the spectral densities of the individual layers were measured with a multispectral imaging system (*Perkin Elmer* – *Vectra 3.0*) coupled with the microscope. The contamination factors for the Agfacolor were derived integrating the products of the spectral densities and the spectral bands: $cf_1 = 0.390$, $cf_2 = 0.116$ and $cf_3 = 0.125$.

The original unfaded colors of the Agfacolor film are not known; hence the reference image for the automatic color correction (cf. section V) was obtained with a ‘manual’ correction that gave a plausible color balance to the image. The minimization of the color difference was not based on all pixels; it was instead based on a subset of pixels that were likely to be achromatic in the original film before fading, i.e. the stone paver and the white tarp over the fruit stand (see Fig. 5). We imagine that the vegetables and clothes were the most colorful elements of the original image; these elements were not considered by the computer routine to identify the optimal LUTs, so their original tints were “free to emerge” where residual color information was present.

The automatic color correction of the Agfacolor was run on the simple merge image ($IMG_R - IMG_G - IMG_B$) and on the image resulting from the dye purification procedure ($IMG_{cyan} - IMG_G - IMG_B$). A detail of the two unfaded images is reported in Fig. 6. The dye purification procedure produces an image with more saturated colors, as for instance the orange vegetables on the right (carrots?), the red vegetables in the middle (beetroots?), and the blue-striped shirt of the man. The vegetables in the cardboard box on the left (white asparagus?), on the other hand, remain colorless.



Fig. 6. Result of the digital unfading for a detail of the analyzed Agfacolor film frame: reconstructed colors from the “simple merge” image (top), and from the “pure merge” image (bottom).

VIII. CONCLUSION

The dye purification allows extracting the residual color information of the cyan dye in a faded chromogenic film. The digital processing of the image resulting from the dye purification procedure provides a more effective color restoration.

In the presented case studies, the images were processed with 1D-LUTs only, which adjust contrast, whitepoint and color balance, while they do not directly affect the colors saturation. Therefore, the colors of the restored images are not the result of an arbitrary *colorization*: the dye purification just brings back residual color information that is still present in the film.

The calculations for the dye purification require the knowledge of the spectral densities of the individual dyes of the film. Spectroscopic measurements in thin section provided convincing results, but they need complex equipment and experienced laboratory technicians to be carried out. By publishing the spectroscopic measurements on the *Timeline of Historical Film Colors* [14] we will provide a possibility for other researchers to carry out the dye purification method without the invasive and difficult procedure of cutting thin sections from the film.

ACKNOWLEDGMENT

The authors would like to thank Claudia Meyer of the Institute of Anatomy, Karina Silina of the Institute of Experimental Immunology, Andres Käch, Ursula Lüthi and Carmen Kaiser of the Center for Microscopy and Image Analysis, all from the University of Zurich.

Anke Mebold, film archivist and restorer at the Deutsches Filminstitut - DIF, provided the film used in the experiments.

REFERENCES

- [1] H. Wilhelm and C. Brower, *The Permanence and Care of Color Photographs: Traditional and Digital Color Prints, Color Negatives, Slides, and Motion Pictures*. Grinnell, IA, USA: Preservation Publishing Company, 1993, pp. 299–344.
- [2] L. Rosenthaler, A. Wittmann, A. Günzl, and R. Gschwind, "Restoration of old movie films by digital image processing," in *Proc. IMAGECOM'96*, Bordeaux, France, 1996.
- [3] M. Chambah and B. Besserer, "Digital color restoration of faded motion pictures," in *Proc. International Conference on Color in Graphics and Image Processing (CGIP'2000)*, Saint-Étienne, France, 2000.
- [4] A. Rizzi, C. Gatta, C. Slanzi, G. Ciocca, and R. Schettini, "Unsupervised color film restoration using adaptive color equalization," in *Visual Information and Information Systems. VISUAL 2005. Lecture Notes in Computer Science*, vol. 3736, Berlin-Heidelberg: Springer, 2006.
- [5] G. Trumphy and B. Flueckiger, "Light source criteria for digitizing color films," in *Proc. 2015 Colour and Visual Computing Symposium (CVCS)*, Gjøvik, Norway, 2015, pp. 1–5.
- [6] W.T. Hanson JR, "Color correction with colored couplers," *Journal of the Optical Society of America*, vol. 40, no. 3, pp. 166–171, 1950.
- [7] B. Flueckiger et al., "Investigation of Film Material-Scanner Interaction," Zurich, Report Ver. 1.1., Feb. 2018. [Online]. Available: <https://diastor.ch/results/#SCAN>, Accessed on: Apr. 9, 2018
- [8] G. Trumphy and R. Gschwind, "Conflicting Colors: Film Scanning versus Film Projection," in *Proc. 25th Color and Imaging Conference*, Lillehammer, Norway, 2017, pp. 188–191.
- [9] Colorimetry – Technical report, Commission internationale de l'éclairage, CIE 15, 2004.
- [10] A. Stockman and L. T. Sharpe, "Spectral sensitivities of the middle- and long-wavelength sensitive cones derived from measurements in observers of known genotype," *Vision Research*, vol. 40, no. 13, pp. 1711–1737, June 2000.
- [11] J. C. Lagarias, J. A. Reeds, M. H. Wright, and P. E. Wright, "Convergence Properties of the Nelder-Mead Simplex Method in Low Dimensions," *SIAM J. Optim.*, vol. 9, no. 1, pp. 112–147, 1998.
- [12] Colorimetry, Part 4: CIE 1976 L*a*b* Colour Space – Standard, Commission internationale de l'éclairage, CIE S 014-4/E, 2007.
- [13] R. Gschwind, E. Zbinden, G. Trumphy, and J. K. Delaney, "Color negatives at the demise of silver halides," in *ICOM-CC 18th Triennial Conference Preprints*, Copenhagen, Denmark, art. 1401.
- [14] B. Flueckiger. (2012) *Timeline of Historical Film Colors*. [Online]. Available: <http://zauberklang.ch/filmcolors/>